

REPORT NO. DOT - TSC - FAA - 71 - 6

*Hagcroft*

# **COLLISION RISK MODEL FOR NAT REGION**

**RONALD HERSHKOWITZ  
TRANSPORTATION SYSTEMS CENTER  
55 BROADWAY  
CAMBRIDGE, MA. 02142**

**MAY 1971  
TECHNICAL REPORT**



AVAILABILITY IS UNLIMITED. DOCUMENT MAY BE RELEASED  
TO THE NATIONAL TECHNICAL INFORMATION SERVICE,  
SPRINGFIELD, VIRGINIA 22151, FOR SALE TO THE PUBLIC.

**Prepared for  
FEDERAL AVIATION ADMINISTRATION  
WASHINGTON, D.C. 20590**



1. Report No.	2. Government Accession No.	3. Recipient's Catalog No.	
4. Title and Subtitle Collision Risk Model for NAT Region		5. Report Date May 1971	6. Performing Organization Code PSA
7. Author(s) Ronald Hershkowitz	8. Performing Organization Report No. DOT-TSC-FAA-71-6		
9. Performing Organization Name and Address Transportation Systems Center 55 Broadway Cambridge, Mass., 02142		10. Work Unit No. R-1032	11. Contract or Grant No. FA-04
12. Sponsoring Agency Name and Address Federal Aviation Administration Washington, D. C. 20590		13. Type of Report and Period Covered Technical Report	
14. Sponsoring Agency Code			
15. Supplementary Notes  Reprint of Report dated November, 1970			
16. Abstract This paper reviews and summarizes the essential features of the collision risk model used to analyze the effects of separation standards on safety for the parallel tracking system employed in the North Atlantic. The derivation of the model is traced from a set of basic assumptions to formulation of various philosophies and a brief set of conclusions and recommendations for future work. Section VII contains a complete reference list.			
17. Key Words Collision Risk Model Composite Problem Vertical Separation Lateral Separation		18. Distribution Statement  Unclassified-Unlimited	
19. Security Classif. (of this report) Unclassified	20. Security Classif. (of this page) Unclassified	21. No. of Pages 55	22. Price



Table of Contents

	<u>Page</u>
I. Introduction. . . . .	1
II. General Derivation. . . . .	3
A. Modeling Assumptions. . . . .	3
B. Derivation Outline. . . . .	5
C. Collision Rate (Lateral & Vertical) . . . . .	8
D. Proximity Times . . . . .	17
E. Collision Risk (Lateral & Vertical) . . . . .	22
III. Model Extensions. . . . .	23
A. Composite Risk. . . . .	23
B. Longitudinal Risk . . . . .	24
C. Number of Accidents . . . . .	26
IV. Parameter Evaluation. . . . .	29
A. Nature of Parameter Estimates . . . . .	29
B. Definitions . . . . .	31
C. NAT SPG Parameter Values. . . . .	34
D. Overlap Probability, $P_Y(S_Y)$ . . . . .	34
V. Results . . . . .	42
VI. Conclusions and Recommendations . . . . .	48
VII. References. . . . .	51



## I. Introduction

This paper reviews and summarizes the essential features of the collision risk model used to analyze the effects of separation standards on safety for the parallel tracking system employed in the North Atlantic. This model was originated by P.G. Reich<sup>1,2,3</sup> of the United Kingdom and has been refined and extended by the North Atlantic Systems Planning Group (NAT SPG)<sup>4-8</sup>, a study group set up under the auspices of ICAO.

Section II derives the model from a set of basic assumptions. The assumptions are discussed and the derivation procedure is outlined. The collision risk due to loss of lateral separation and the risk due to loss of vertical separation are derived.

Section III serves to extend the results derived in Section II. First, we investigate two additional cases of interest: (1) the accident rate due to longitudinal (along-track) failure and (2) the accident rate due to a simultaneous loss in both vertical and lateral separation (i.e. the composite problem). Then, we relate the risk function to the expected number of accidents in 10 million flying hours,  $N_a$ , a convenient function in terms of selecting safety criterion. (A complete list of the principal relationships of interest are presented.)

Next, in Section IV, the various philosophies used in obtaining parameter estimates are discussed with respect to the solution method. The parameters of interest are defined and categorized. Present parametric values are noted along with their source. Special emphasis is placed on the methods used to model the tail area and tail shape of the aircraft position density.

Section V contains a summary of the principal NAT SPG results derived to date.

Section VI closes the current discussion of the NAT SPG collision risk model with a brief set of conclusions and recommendations for future work.

Section VII contains a complete reference list for those who wish to pursue the entire question in more detail.



## II. General Derivation

### A. Modeling Assumptions

(i) Air-Space: The principal region of the North Atlantic (NAT) being considered extends from roughly  $18^{\circ}\text{W}$  to  $50^{\circ}\text{W}$  longitude and from  $45^{\circ}\text{N}$  to  $61^{\circ}\text{N}$  latitude. A parallel tracking system is employed whereby each aircraft is cleared to fly down "tubes", nominally centered at specific vertical and lateral positions. The separation distance between the center lines of these usable tracks are chosen in order to maintain safety standards in the vertical and lateral directions. Similarly, the allowable times for aircraft entering a particular track are set in accordance with along-track safety requirements. We will be discussing two such parallel systems: (1) the conventional, and (2) the composite. In the conventional, or rectangular system, each flight path has two vertical and two lateral neighbor paths (neglecting "edge" effects). The composite system path is bordered by four diagonal paths in addition to the two vertical and two lateral found in the conventional system. (In essence, the composite system can be viewed as two rectangular systems offset from one other by half a standard separation in each dimension). These two systems are represented in Figure 1a and 1b where only unidirectional flow is represented for the time being. We have taken a cross-sectional slice perpendicular to the along track direction.)

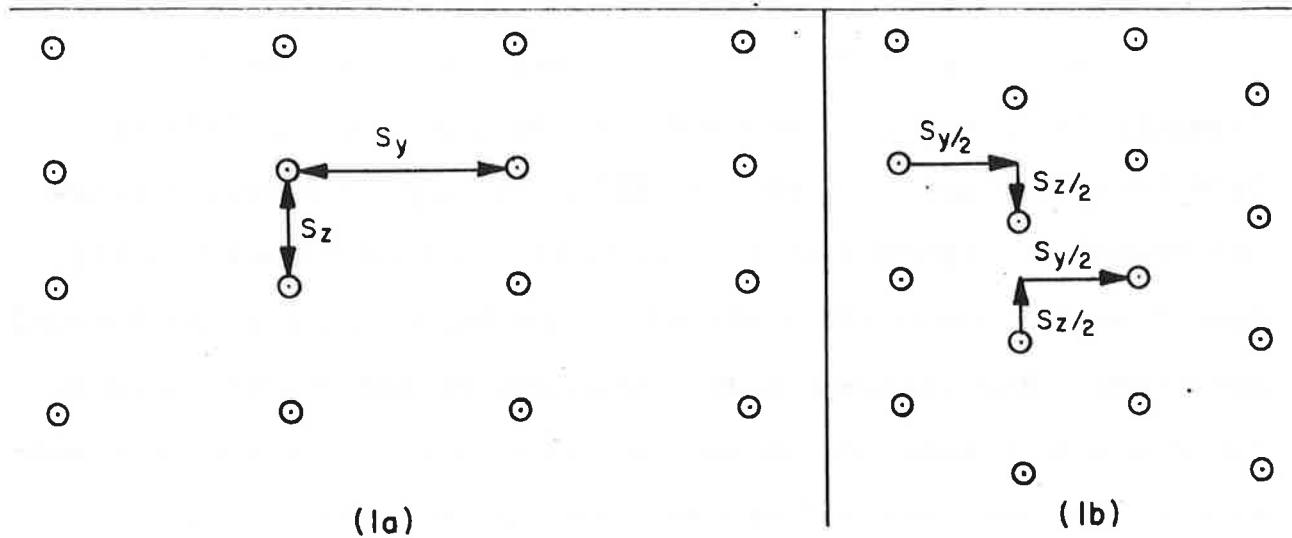


Figure 1.- Tracking Systems  
 (a): Conventional  
 (b): Composite

(ii) Collision Avoidance: No provision is made in the model for collision avoidance following a visual or instrument sighting of another aircraft. Since pilot initiated evasive action is more likely to prevent an accident than cause one, this is considered a conservative assumption.

(iii) Dimensional Independence: The flying errors in each dimension are assumed to be independent of one another. A careful study of the data will be required in order to analyze the effect of this assumption on the final results.

(iv) Aircraft Independence: The flying errors between neighboring aircraft are assumed to be independent. There are

a variety of ambient conditions (such as weather and external navigation aids) which tend to cause correlated bias errors between neighboring aircraft. Hence this assumption, too, is considered to be conservative in nature.

#### B. Derivation Outline

The derivation of the collision risk equation depends on a clear understanding of three key concepts: (1) the separation vector, (2) the collision slab and (3) the proximity shell.

At any given time during a flight, an aircraft is assumed to be at a given position. The true position will be somewhat displaced from this intended position due to flying errors. We can represent both the intended and the actual positions of two aircraft with respect to each other by time-varying separation vectors. An example of this representation is given in Figure 2 (for a fixed time).

Since we assume that intended flight paths are designed to be non-intersecting, collisions result solely from the AA' and BB' offsets caused by flying errors. A collision will occur when one aircraft enters within a specific distance of another. To be mathematically precise, this distance is defined in terms of the collision slab, depicted in Figure 3.

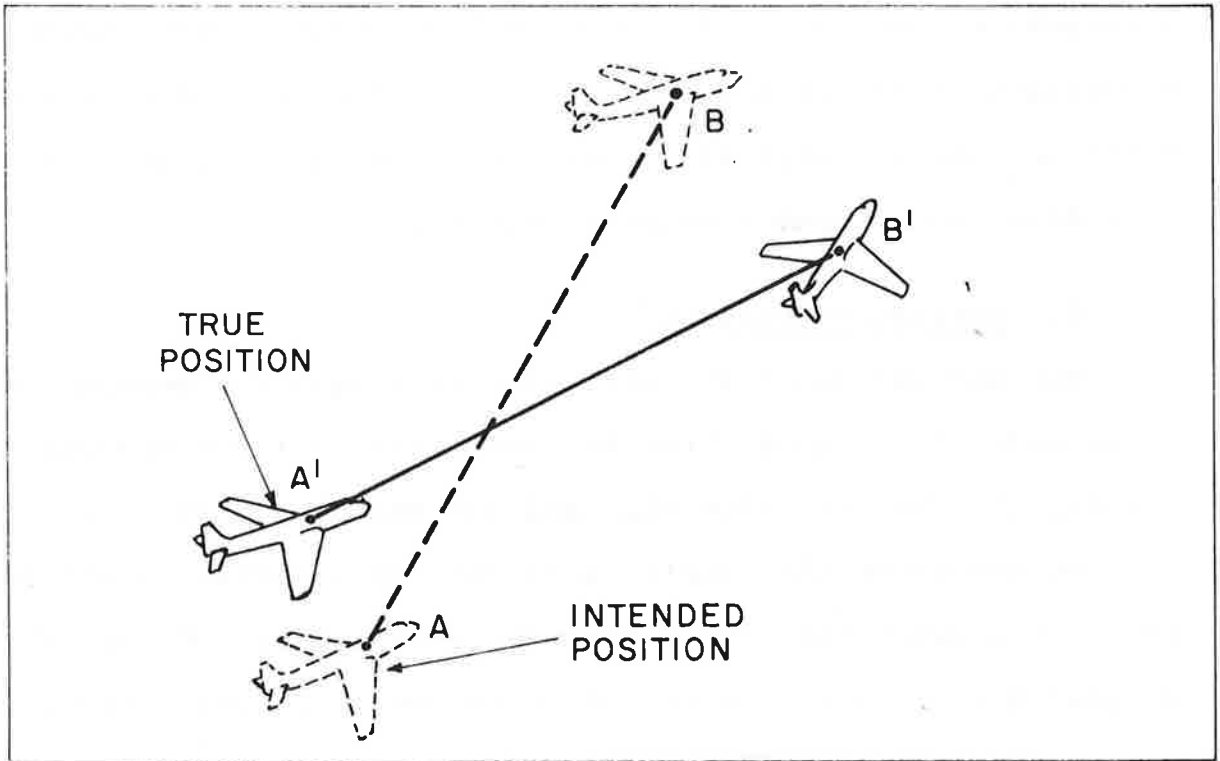


Figure 2.- Separation Vectors

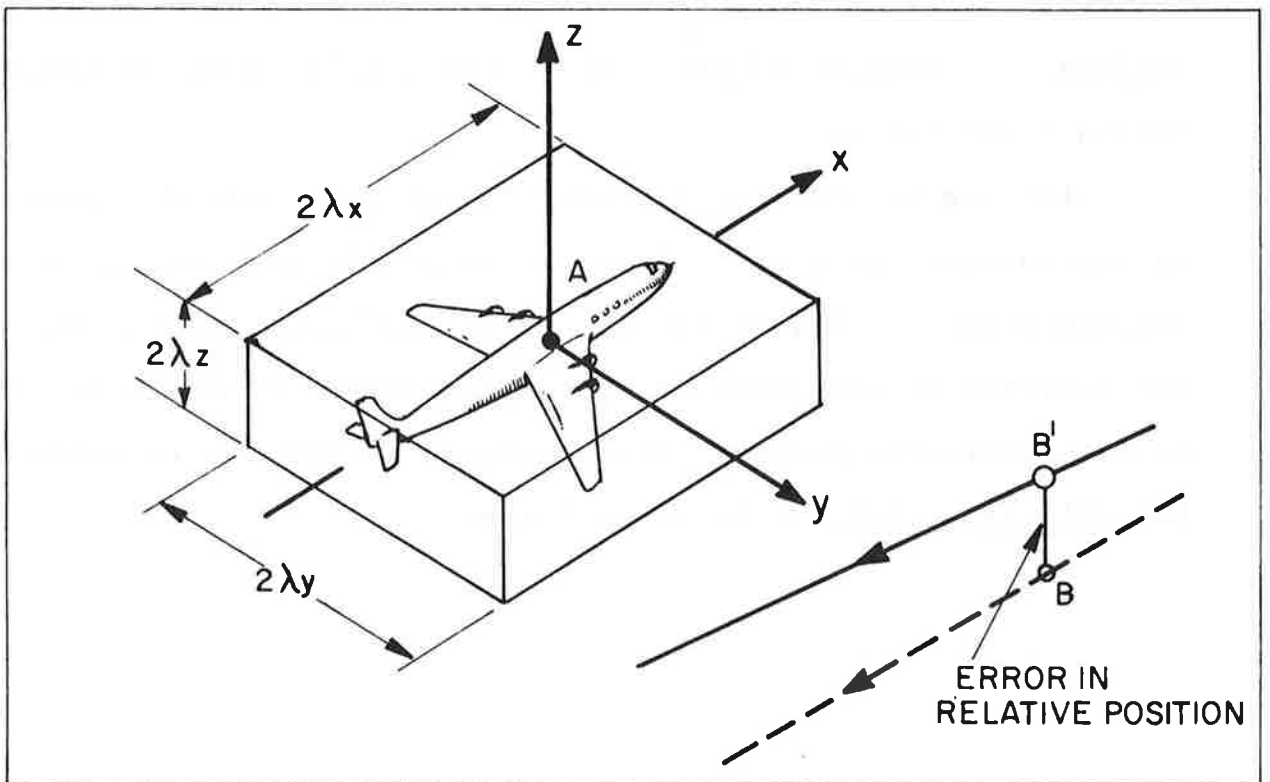


Figure 3.- Collision Slab

The dimensions,  $\lambda_x$ ,  $\lambda_y$ , and  $\lambda_z$  are nominally taken to be the metallic dimensions of the aircraft, although the slab can be extended to include the effect of vortices.

Not all pairs of aircraft pose threats to each other. Only those aircraft nominally close enough to be drawn, with some threshold probability, to within collision slab dimensions as a result of flying errors, are considered as potential hazards to one another. This directly leads to the concept of a proximity shell (shown in Figure 4.)

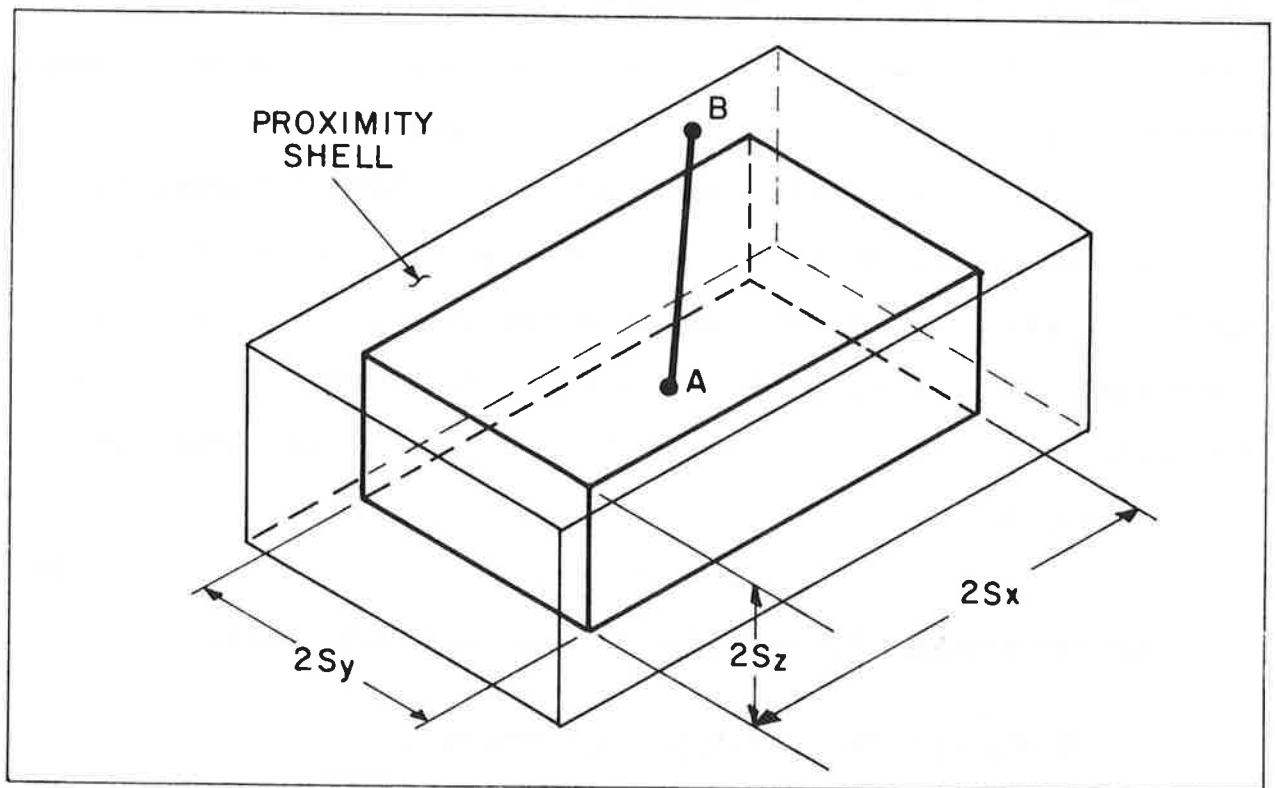


Figure 4.- Exposure to Risk

A significant risk will occur only if one aircraft has an intended flight path which enters, or is close to, the proximity shell of another. Risk is assumed to fall off rapidly outside the shell. The proximity shell dimensions,  $S_x$ ,  $S_y$  and  $S_z$ , must be such that there is no meaningful probability that flying errors can result in a collision between two aircraft which never enter each other's shell. For the parallel tracking system being considered, the exposure dimensions are taken as the track separation dimensions. In other words, we will assume an aircraft is exposed to a risk from, or is "proximate to", all other aircraft whose intended paths are no more than one respective separation distance apart in any direction.

The problem will be considered in two parts. First, we will assume two aircraft are proximate and calculate their collision rate, CR, the number of collisions per unit of proximate time. Secondly, we will calculate the proximity time, T. The final risk then, will simply be the product of these two quantities, or,

$$\text{RISK} = \text{CR} \times \text{T} \quad (1)$$

We now proceed by calculating the collision rate.

### C. Collision Rate (Lateral & Vertical)

The collision rate, as we have defined it, is the rate at which one aircraft will enter the collision slab (Figure 3) of another aircraft, given it has already entered its proximity shell (Figure 4). This rate will obviously be a function of the

time-varying vector describing the intended relative positions of the two aircraft. Each vector [AB] (shown in Figure 2 for a given instant of time) will result in a different collision rate. Therefore, we must calculate the rate for each [AB],  $CR_{[AB]}$ , and then sum over all the possible vectors.

Taking the motion of one aircraft relative to the other, the collision process may be looked on as a particle bombarding a slab. The collision rate is given by the expected number of times the particle shown at B' in Figure 3 enters the slab through (1) the sides, (2) the ends and (3) the top and bottom. The total rate is then found by summing these contributions.

We define the following quantities:

$N_x$  is the expected frequency with which the along-track separation shrinks to less than  $\lambda_x$ .

$N_y$  and  $N_z$  are similarly defined for, respectively, the across-track and vertical directions.

$P_x$  is the probability that the along-track separation is less than  $\lambda_x$ , i.e. the proportion of time the aircraft spend in this condition.

$P_y$  and  $P_z$  are similarly defined for, respectively, the across-track and vertical direction.

Suffix [AB] denotes values which the above quantities take throughout periods when the planned separation may be taken as sensibly constant at the vector [AB].

The frequency with which the particle B enters the slab through either end is given by the probability that its y and z coordinates lie within the dimensions  $\lambda_y$  and  $\lambda_z$  of the end faces multiplied by the frequency with which its x coordinates becomes less than  $\lambda_x$ . For the constant intended separation [AB], this may be written as,

$$(N_{x^y^z} P_{y^z} P_z) [AB]$$

Similarly, the frequency of entering the slab through either side is given by

$$(N_{y^x^z} P_{x^z} P_z) [AB]$$

Finally, the frequency of entering the slab through the top or bottom is given by

$$(N_{z^y^x} P_{y^x} P_x) [AB]$$

Therefore, the total collision rate, for the intended separations vector [AB], obtained by summing the above quantities, is

$$(CR) [AB] = (N_{x^y^z} P_{y^z} P_z) [AB] + (N_{z^x^y} P_{x^y} P_y) [AB] + (N_{y^z^x} P_{z^x} P_x) [AB] \quad (2)$$

The frequency with which the  $r^{\text{th}}$  coordinate (where r represents x, y or z) becomes less than  $\lambda_r$  is equal to the proportion of time the  $r^{\text{th}}$  dimension is less than  $\lambda_r$  divided by the average duration of this event. Denoting  $t_r$  as this average duration:

$$N_r = \frac{P_r}{t_r} \quad (3)$$



Alternately, then, we may represent the collision rate by equation (4) below:

$$(CR)_{[AB]} = P_x P_y P_z \left( \frac{1}{t_x} + \frac{1}{t_y} + \frac{1}{t_z} \right) \quad (4)$$

We can relate the relative frequency of overlap in the  $r^{\text{th}}$  direction,  $N_r$ , to the probability of overlap in the  $r^{\text{th}}$  direction,  $P_r$ , in a more mathematically rigorous fashion by considering the following derivation:

DERIVATION 1:

Let  $G_{[AB]}(r, \dot{r})$  be the joint density function for two aircraft, nominally separated by vector  $[AB]$ , having a relative velocity  $\dot{r}$  and being separated by a distance  $r$  (i.e.,  $G_{[AB]}(r, \dot{r}) dr d\dot{r}$  is the proportion of time that the separation in the  $r^{\text{th}}$  dimension lies between  $r$  and  $r + dr$  and is changing at a rate between  $\dot{r}$  and  $\dot{r} + d\dot{r}$ .) The time taken for the separation in the  $r^{\text{th}}$  direction to change from  $r$  to  $r \pm dr$  is

$$\frac{dr}{|\dot{r}|}$$

From Equation (3), the average frequency with which the separation passes through the element  $(r, r + dr)$  is when the velocity is in the range from  $\dot{r}$  to  $\dot{r} + d\dot{r}$ , is

$$\frac{G_{[AB]}(r, \dot{r}) dr d\dot{r}}{\frac{dr}{|\dot{r}|}} = |\dot{r}| G_{[AB]}(r, \dot{r}) d\dot{r}$$

The total frequency of passing from  $r$  to  $r + dr$  is found by integrating over all

$$\int_{-\infty}^{\infty} |\dot{r}| G_{[AB]}(r, \dot{r}) d\dot{r}$$

Since the function  $G_{[AB]}(\dot{r}, r)$  is likely to change only slightly over an interval of twice the collision dimension,  $\lambda_r$ , we can approximate the total frequency of passing into the slab in the  $r^{\text{th}}$  direction,  $(N_r)_{[AB]}$ , by

$$(N_r)_{[AB]} = \int_{-\infty}^{\infty} |\dot{r}| G_{[AB]}(0, \dot{r}) d\dot{r} \quad (5)$$

In the case of  $r$  and  $\dot{r}$  being independent (an assumption which will be commented upon in Section IV), we have

$$(N_r)_{[AB]} = \phi_{[AB]}(0) |\bar{\dot{r}}| \quad (6)$$

where  $\phi_{[AB]}(r)$  is the density function for  $r$  alone.

The probability of overlap  $P_r{}_{[AB]}$ , is simply the probability that  $|r| \leq \lambda_r$ . Therefore

$$P_r{}_{[AB]} = \int_{-\lambda_r}^{\lambda_r} \phi(r) dr \doteq \int_{-\lambda_r}^{\lambda_r} \phi(0) dr$$

and,

$$(P_r)_{[AB]} \doteq 2\lambda_r \phi_{[AB]}(0) \quad (7)$$

Comparing equations (6) and (7), we arrive at the desired result:

$$N_{r[AB]}(S_r) = \overline{|\dot{r}(S_r)|} P_{r[AB]}(S_r) / 2\lambda_r \quad (8)$$

where the intended r separation,  $S_r$ , is explicitly noted. This result is not very surprising. Comparing equation (7) to equation (2), our intuition is satisfied by noting that,

$$t_r = \frac{2\lambda_r}{|\dot{r}|} \quad (9)$$

or, in words, the average time spent by a particle in the collision slab is simply the total distance it travelled while traversing the slab divided by its average speed. This completes derivation 1.

Thus far, our derivation has been quite general. It provides the framework for calculating the collision rate between two aircraft regardless of the orientation of their intended tracks. We now wish to specialize our problem by considering the parallel tracking system presently in operation over the North Atlantic. Furthermore, we initially concentrate on the rectangular system depicted in Figure 1a, deferring the composite calculations until Section III.

The rectangular system has a special feature, namely, that the intended separation between proximate aircraft in the lateral

(y) and the vertical (z) direction remain constant throughout their respective flights. Therefore, the  $P_y$ ,  $P_z$ ,  $N_y$ , and  $N_z$  dependence on the vector [AB], can be suppressed and equation (2) can be more conveniently written as,

$$(CR)_{[AB]} = (N_x)_{[AB]} P_x P_y + (P_x)_{[AB]} (N_y P_z + P_y N_z) \quad (10)$$

A collision can occur as a result of one of the following three occurrences: (1) a loss in the vertical separation between two aircraft flying on the same lateral path, (2) a loss in the lateral separation between aircraft occupying the same flight level and (3) a loss in the longitudinal separation between those aircraft sharing the same nominal lateral and vertical positions. The total collision risk is the sum of these three effects (which are assumed to be independent.) The longitudinal case involves special considerations, not found to the lateral and vertical derivation, and is temporarily deferred.

The collision rate due to a loss in lateral separation (to be referred to as the lateral rate) is denoted by  $CR_{Y[AB]}$ . It is obtained directly from equation (10) by explicitly noting the fact that the parameters of interest, the N's and P's must be calculated by initially assuming a nominal vertical separation of 0 feet and a nominal lateral separation represented by some standard separation,  $S_y$ . Therefore,

$$(CR_Y)_{[AB]} = (N_x)_{[AB]} \left[ P_y (S_y) P_z (0) \right] + (P_x)_{[AB]} \left[ P_y (S_y) N_z (0) + N_y (S_y) P_z (0) \right] \quad (11)$$

Analogously, the vertical risk,  $CR_z$ , is equal to:

$$\begin{aligned} (CR_z)_{[AB]} &= (N_x)_{[AB]} \left[ P_Y(0) P_Z(S_z) \right] \\ &+ (P_x)_{[AB]} \left[ P_Y(0) N_Z(S_z) + N_Y(0) P_Z(S_z) \right] \end{aligned} \quad (12)$$

Theoretically, we must now analyze equations (11) and (12) for each possible x direction projection of the vector [AB] and then integrate the result. The longitudinal separations are not structured as explicitly as are the vertical and lateral (see Section III) and this approach is not practically feasible. Instead, we analyze the aggregate behavior of the traffic in a statistical manner.

The longitudinal separation between aircraft on adjacent tracks are assumed to be independent. This is a good assumption since, operationally, permission to enter the system on a given track is a function of the last entry time on that particular track and is independent of the traffic on adjacent tracks. Given proximity, then, the probability of overlap in the x direction is simply the ratio of the x dimension of the collision slab,  $2\lambda_x$ , to the x dimension of the proximity shell,  $2S_x$ .

$$(P_x)_{[AB]} = \frac{\lambda_x}{S_x} \quad (13)$$

The relative frequency can be expressed by combining equations (13) and (8),

$$(N_x)_{[AB]} = \frac{|\dot{x}|}{2S_x} \quad (14)$$

Substituting equations (13) and (14) into equations (11) and (12), the collision rates due to lateral and vertical separation losses are given by

$$CR_Y = \frac{1}{S_X} \left\{ \frac{|\dot{\bar{x}}|}{2} P_Y(S_Y) P_Z(0) + \lambda_X P_Y(S_Y) N_Z(0) + \lambda_X N_Y(S_Y) P_Z(0) \right\} \quad (15)$$

and,

$$CR_Z = \frac{1}{S_X} \left\{ \frac{|\dot{\bar{x}}|}{2} P_Y(0) P_Z(S_Z) + \lambda_X P_Y(0) N_Z(S_Z) + \lambda_X N_Y(0) P_Z(S_Z) \right\} \quad (16)$$

Introducing equation (8) into the above relationships allows us to express the rate function directly in terms of the velocities and hazard distances.

One last comment on the lateral and vertical rates concerns directivity.  $|\dot{\bar{x}}|$  is the average relative along-track velocity between two aircraft not on the same track and level. Obviously, its value will depend on whether the two aircraft are travelling in the same or opposite directions. For same direction traffic,

$$|\dot{\bar{x}}| = \overline{\Delta V} \quad (17)$$

where  $\overline{\Delta V}$  is the average difference in their velocities. For opposite-direction traffic, we let

$$|\dot{\bar{x}}| = \overline{2V} \quad (18)$$

where  $\overline{V}$  represents the velocity of each aircraft (assumed equal for the moment). Substitution of these values for  $|\dot{\bar{x}}|$  into equations (15) and (16) results in separate rate functions for same and opposite direction flow.

D. Proximity Times

As mentioned on page 7, the derivation of the collision risk function is a two step process. Part C of this section was devoted to deriving expressions for the collision rate or number of collisions per unit proximity time. We now address ourselves to the problem of calculating the expected proximity time. In keeping with the procedure developed in the rate analysis, we will consider the lateral proximity and the vertical proximity separately. The conditions necessary for proximity are reviewed in Figure 5 below.

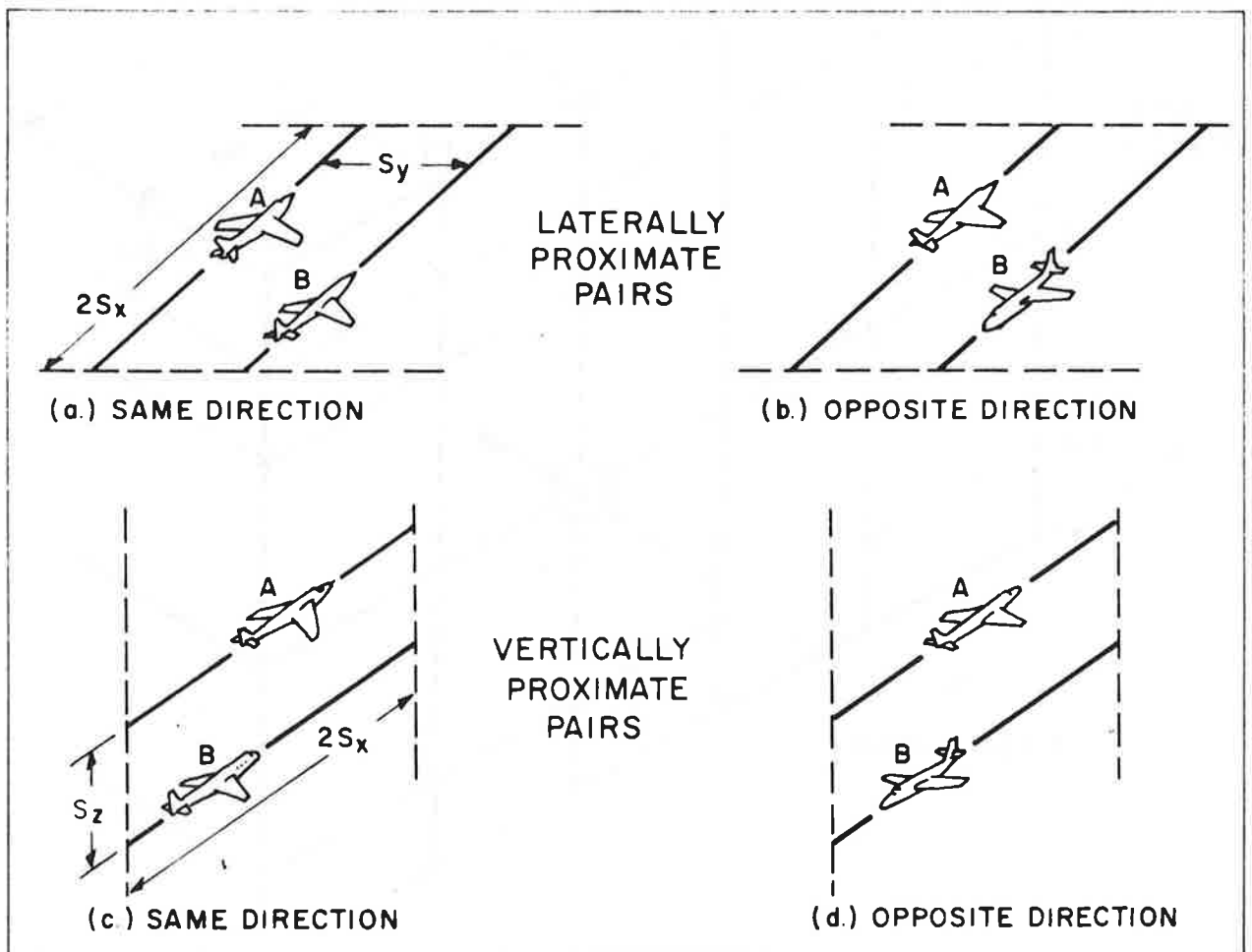


Figure 5.- Proximity Pairs

We begin by calculating the lateral proximity time. To be laterally proximate, two aircraft must be assigned to adjacent lateral lanes at the same flight level and be within longitudinal proximity of one another. This condition is indicated in parts (a) and (b) of Figure 5.

A cross-section of a typical tracking section is presented in Figure 6.

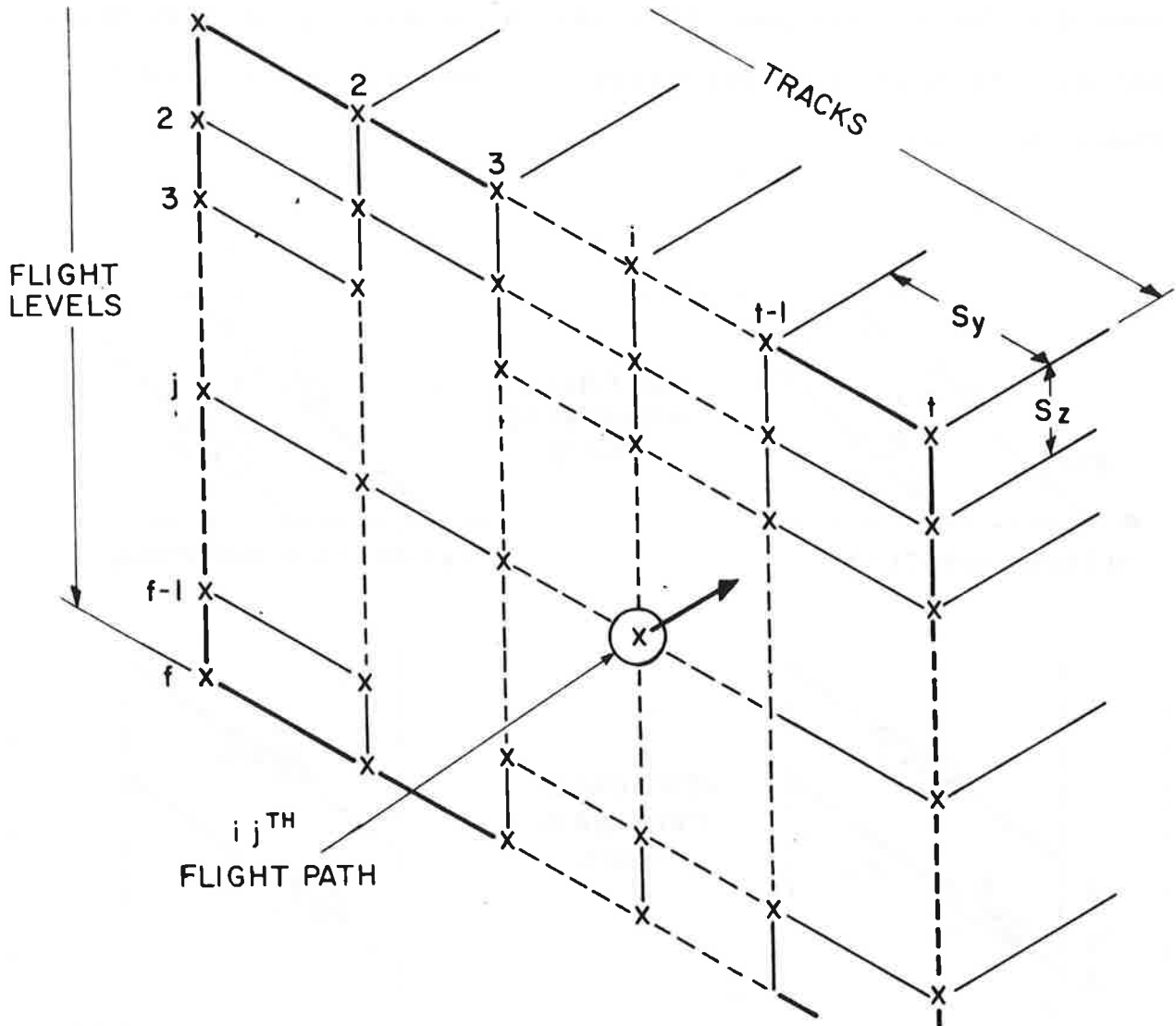


Figure 6.- Tracking System (3 Dimensional View)



The  $(i,j)^{th}$  track has associated with it a flow rate of  $m_{ij}$  aircraft per hour. The average density of aircraft (aircraft per nmi) on the  $(i-1, j)^{th}$  track is,

$$\frac{m_{i-1,j}}{\bar{V}}$$

where  $\bar{V}$  is the average velocity of the aircraft. At any instant of time, the expected number of aircraft on track  $(i-1, j)$  that are proximate to, or within  $\pm S_x$  of, a given aircraft on track  $(i, j)$  is given by,

$$\frac{2S_x m_{i-1,j}}{\bar{V}}$$

The time required to complete a trip along an L nmi tracking system is  $L/\bar{V}$ . Therefore, per trip, the expected length of time during which an  $(i,j)^{th}$  track aircraft is proximate to an aircraft in the  $(i-1, j)^{th}$  track, is simply:

$$\frac{2S_x m_{i-1,j}}{\bar{V}} \cdot \frac{L}{\bar{V}}$$

In order to establish the total number of proximate pairs existing between lateral lanes  $i$  and  $i-1$  on flight level  $j$ , we multiply the above expression by the flow rate for track  $(i, j)$ . Therefore

$$\left\{ \begin{array}{l} \text{Time of exposure of proximate pairs on tracks} \\ \text{(i-1, j) and (i, j)/unit} \\ \text{time of operation} \end{array} \right\} = \frac{2LS_x}{\bar{V}^2} m_{i-1,j} m_{i,j} \quad (19)$$

Summing the result of equation (19) over all pairs of adjacent lateral lanes yields,

$$\dot{T}_Y = \frac{2L S_x}{\bar{V}^2} \sum_{i=2}^t \sum_{j=1}^f m_{i-1,j} m_{i,j} \quad (20)$$

where  $\dot{T}_y$  is the total number of proximate lateral pairs per hour of flight. Letting H represent the total number of flying hours being considered, the lateral proximity time,  $T_y$ , is given by equation (21).

$$T_y = \frac{2HLS_x}{\bar{V}^2} \sum_{i=2}^t \sum_{j=1}^f m_{i-1,j} m_{i,j} \quad (21)$$

Similarly, it can be shown that the vertical proximity time is given by

$$T_z = \frac{2HLS_x}{\bar{V}} \sum_{j=2}^f \sum_{i=1}^t m_{i,j-1} m_{i,j} \quad (22)$$

The only difference between the two expressions (equations (21) and (22)), is the order to summation.

Just as directivity was an issue in calculating the collision rate, so it is with the calculation of the proximity time. Each proximity is classified as either a same-direction or an opposite-direction proximity depending on the respective flows on the adjacent tracks being considered. (The flow in any given track is, of course, unidirectional.) The proximity calculations for each case are segregated and summed separately. Figure 6 indicates all traffic flowing into the paper. Hence, equations (21) and (22) are correct in terms of Figure 6 and represent same-direction proximity.

In general, however, equations (21) and (22) can be specialized as below:

$$T_Y(\text{same}) = \frac{2HLS_x}{\bar{V}^2} \sum_{\substack{\text{Same level} \\ \text{Adjacent lanes} \\ \text{Same-direction traffic}}} \sum m_{i-1,j} m_{i,j} \quad (23)$$

$$T_Y(\text{opp}) = \frac{2HLS_x}{\bar{V}^2} \sum_{\substack{\text{Same level} \\ \text{Adjacent lanes} \\ \text{Opposite-direction traffic}}} \sum m_{i-1,j} m_{i,j} \quad (24)$$

$$T_Z(\text{same}) = \frac{2HLS_x}{\bar{V}^2} \sum_{\substack{\text{Same lateral lane} \\ \text{Adjacent levels} \\ \text{Same-direction traffic}}} \sum m_{i,j-1} m_{i,j} \quad (25)$$

$$T_Z(\text{opp}) = \frac{2HLS_x}{\bar{V}^2} \sum_{\substack{\text{Same lateral lane} \\ \text{Adjacent levels} \\ \text{Opposite-direction traffic}}} \sum m_{i,j-1} m_{i,j} \quad (26)$$

One conclusion to be drawn from equations (23)-(26) is that the proximity time is approximately proportional to the square of the traffic intensity. (This is due to the quadratic form of the above expressions with respect to the flow rates, which are themselves proportional to the intensity.) Another conclusion deals with the dependence of the collision risk on the assumed longitudinal proximity standard,  $S_x$ . Equations (15) and (16) show the collision rate to be inversely proportional to  $S_x$ . The proximity time is directly proportional to  $S_x$ . The risk therefore is independent of this standard. The larger the proximity standard, the more planes we will "consider" as being proximate. At the

same time, however, the less likely it is that two proximate aircraft will overlap longitudinally (see equation 12).  $S_x$ , then, is simply a mathematical tool in our analysis.

#### E. Collision Risk (Lateral & Vertical

As previously stated, the collision risk is the product of the proximity time and the collision rate per unit proximity time. The risk for same and oppositely directed aircraft must be calculated separately and summed together. Combining the results of Sections B and C, we obtain the following lateral and vertical risk functions:

$$\begin{aligned}
 CR_Y = & \frac{T_Y \text{ (same)}}{S_x} \left[ \frac{\Delta \bar{V}}{2} P_Y(S_Y) P_Z(0) + \lambda_x P_Y(S_Y) N_Z(0) + \lambda_x N_Y(S_Y) P_Z(0) \right] \\
 & + \frac{T_Y \text{ (opp)}}{S_x} \left[ \bar{V} P_Y(S_Y) P_Z(0) + \lambda_x P_Y(S_Y) N_Z(0) + \lambda_x N_Y(S_Y) P_Z(0) \right]
 \end{aligned} \tag{27}$$

where  $T_Y$  (same) and  $T_Y$  (opp) are given explicitly in equations (22) and (23), respectively. Similarly,

$$\begin{aligned}
 CR_Z = & \frac{T_Z \text{ (same)}}{S_x} \left[ \frac{\Delta \bar{V}}{2} P_Y(0) P_Z(S_Z) + \lambda_x P_Y(0) N_Z(S_Z) + \lambda_x N_Y(0) P_Z(S_Z) \right] \\
 & + \frac{T_Z \text{ (opp)}}{S_x} \left[ \bar{V} P_Y(0) P_Z(S_Z) + \lambda_x P_Y(0) N_Z(S_Z) + \lambda_x N_Y(0) P_Z(S_Z) \right]
 \end{aligned} \tag{28}$$

where  $T_Z$  (same) and  $T_Z$  (opp) are given explicitly in equations (24) and (25), respectively.

Alternate forms may be obtained by substituting equation (8) into the above relationships.

### III. Model Extensions

#### A. Composite Risk

The composite collision risk is defined as the probability of collision between two aircraft nominally separated by half a separation standard in both the lateral and vertical dimension ( $S_y/2$  and  $S_z/2$ , respectively). The derivation of the composite risk function is analogous in form to the analysis used for the lateral and vertical cases. There are two sets of modifications in content. (1) The frequency functions ( $N_y$  and  $N_z$ ) and the probability functions ( $P_y$  and  $P_z$ ) are evaluated at the new nominal standards. (2) The proximity times, both same direction,  $T_{yz}$  (same), and opposite direction,  $T_{yz}$  (opp), refer to the proximity caused by nearest diagonal neighbors (see Figure 1). The functional forms for  $T_{yz}$  (same) and  $T_{yz}$  (opp) are the same as equations (25) and (26) except for the need to sum over four, rather than two, lane pairs.

A straightforward extension of our previous results, then, leads to a composite risk given by:

$$\begin{aligned} (CR)_{yz} = & \frac{T_{yz} \text{ (same)}}{S_x} \left[ \frac{\Delta V}{2} P_y \left( \frac{S_y}{2} \right) P_z \left( \frac{S_z}{2} \right) + \lambda_x P_y \left( \frac{S_y}{2} \right) N_z \left( \frac{S_z}{2} \right) + \lambda_x N_y \left( \frac{S_y}{2} \right) P_z \left( \frac{S_z}{2} \right) \right] \\ & + \frac{T_{yz} \text{ (opp)}}{S_x} \left[ \bar{V} P_y \left( \frac{S_y}{2} \right) P_z \left( \frac{S_z}{2} \right) + \lambda_x P_y \left( \frac{S_y}{2} \right) N_z \left( \frac{S_z}{2} \right) + \lambda_x N_y \left( \frac{S_y}{2} \right) P_z \left( \frac{S_z}{2} \right) \right] \end{aligned} \quad (29)$$

## B. Longitudinal Risk

Now consider the case of a collision resulting from a loss in along-track separation. The two aircraft in question are assumed to occupy the same track and, of course, fly in the same direction. Combining equations (8) and (12), the longitudinal rate can be written as function of the separation vector [AB]:

$$\left\{ \begin{array}{l} \text{Longitudinal} \\ \text{Rate} \end{array} \right\} = \left[ \frac{|\dot{x}|}{2\lambda_x} + \frac{|\dot{y}(0)|}{2\lambda_y} + \frac{|\dot{z}(0)|}{2\lambda_z} \right] P_Y(0) P_Z(0) (P_X)_{[AB]}(\cdot) \quad (30)$$

where the argument for  $(P_X)_{[AB]}(\cdot)$  is, as yet, undefined.

In our previous analysis, we were able to drop the [AB] dependence on  $(P_X)_{[AB]}$  by making use of the statistical independence that exists among the longitudinal positions of aircraft occupying adjacent tracks. This independence assumption is no longer valid when considering same-track aircraft. The relative entry times (and, hence, the longitudinal positions) of successive same-track carriers are chosen so as to conform with basic safety standards. This results in a strong correlation between their longitudinal positions.

This correlation, however, is not very well defined. In the lateral and vertical cases, constant nominal separations were assumed to exist between all aircraft pair in the dimensions of interest. The loss in separation, therefore, was a sole function of flying errors. In the longitudinal case, even in the

absence of flying errors, the separation distance between neighboring, same-track aircraft is variable. This is obvious from an operational point of view. Operationally, a minimum entry time is established. An aircraft approaching the gateway to the NAT region will be allowed entry to a particular track only if the required minimum time has elapsed since last entry onto that track. The lack of an infinite reservoir of aircraft entering the system prohibits the uniform adoption of this minimum standard. The nominal distances between aircraft are all in excess of the minimum standard. Within this constraint, however, the nominal separations are random.

These considerations lead us to the weighted-sum approach in solving for  $(P_x)_{[AB]}(\cdot)$  in equation (30). We define the following terms:

$\tilde{P}_x(t)$  is the probability that the along-track separation of a pair of aircraft, initially separated by an amount  $t$  (plus an allowance for Mach number difference), is less than  $\lambda_x$ .

$\tilde{E}_x(t)$  is the average number of aircraft that a given reference aircraft will have on the same track and flight level with initial separation  $t$  (plus an allowance for Mach number difference).

$(P_x)_{[AB]}(\cdot)$  is simply the weighted-sum (or average) of the longitudinal overlap probabilities. Said mathematically,

$$(P_x)_{[AB]}(\cdot) = \sum_t \tilde{E}_x(t) \tilde{P}_x(t) \quad (25)$$

where the sum is taken over all possible initial separations.

Two successive aircraft on the same level and track are always considered to pose a potential threat to one another, and hence are considered to be proximate. Substituting equation (31) to equation (30), therefore yields the risk function itself:

$$(CR)_x = \left[ \frac{|\dot{x}|}{2\lambda_x} + \frac{|\dot{y}(0)|}{2\lambda_y} + \frac{|\dot{z}(0)|}{2\lambda_z} \right] P_y(0)P_z(0) \sum_t \tilde{E}_x(t) \tilde{P}_x(t) \quad (32)$$

### C. Number of Accidents

NAT SPG found the collision risk function to be an inconvenient vehicle with which to establish target levels of safety. The expected number of accidents in 10 million hours of flying time,  $N_a$ , was derived from the collision risk functions, and represents the principal results of the model under discussion. Three minor modifications are necessary in transforming the risk function into the accident function: (1) There are two accidents per collision. Hence multiply (CR) by 2. (2) Divide (CR) by the average number of flying hours over which the proximity times were calculated. This gives us risk per hour. (The value for H is implicit in  $E_x(t)$  and hence is excluded from  $N_{ax}$ .) (3) Multiply the result by  $10^7$  to obtain the desired function. Therefore,

$$N_a = \frac{2 \times 10^7}{H} (CR) \quad (33)$$

The collision risks of interest are given in equations (27), (28), (29), and (32). Substituting equations (8) and (33)



into the above relationships we can summarize the final results as follows:

$$N_{ay} = \frac{2 \times 10^7}{H} P_Y(S_Y) \left[ \frac{T_Y(\text{same})}{S_x} \left( \frac{\Delta \bar{V}}{2} P_Z(0) + \lambda_x N_Z(0) + \frac{\lambda_x \overline{|\dot{Y}(S_Y)|}}{2\lambda_Y} P_Z(0) \right) \right. \\ \left. + \frac{T_Y(\text{opp})}{S_x} \left( \bar{V} P_Z(0) + \lambda_x N_Z(0) + \frac{\lambda_x \overline{|\dot{Y}(S_Y)|}}{2\lambda_Y} P_Z(0) \right) \right] \quad (34)$$

$$N_{az} = \frac{2 \times 10^7 P_Z(S_Z)}{H} \left[ \frac{T_Z(\text{same})}{S_x} \left( \frac{\Delta \bar{V}}{2} P_Y(0) + \lambda_x N_Y(0) + \frac{\overline{|\dot{Z}(S_Z)|} P_Y(0)}{2\lambda_Z} \right) \right. \\ \left. + \frac{T_Z(\text{opp})}{S_x} \left( \bar{V} P_Y(0) + \lambda_x N_Y(0) + \frac{\lambda_x \overline{|\dot{Z}(S_Z)|} P_Y(0)}{2\lambda_Z} \right) \right] \quad (35)$$

$$N_{ayz} = \frac{2 \times 10^7}{H} P_Z\left(\frac{S_Z}{2}\right) P_Y\left(\frac{S_Y}{2}\right) \frac{\lambda_x}{S_x} \left[ T_{YZ}(\text{same}) \left( \frac{\Delta \bar{V}}{2\lambda_x} + \frac{\overline{|\dot{Y}(S_Y/2)|}}{2\lambda_Y} + \frac{\overline{|\dot{Z}(S_Z/2)|}}{2\lambda_Z} \right) \right. \\ \left. + T_{YZ}(\text{opp}) \left( \frac{\bar{V}}{\lambda_x} + \frac{\overline{|\dot{Y}(S_Y/2)|}}{2\lambda_Y} + \frac{\overline{|\dot{Z}(S_Z/2)|}}{2\lambda_Z} \right) \right] \quad (36)$$

and,

$$N_{ax} = 2 \times 10^7 \left[ \frac{\overline{|\dot{x}|}}{2\lambda_x} + \frac{\overline{|\dot{Y}(0)|}}{2\lambda_Y} + \frac{\overline{|\dot{Z}(0)|}}{2\lambda_Z} \right] P_Y(0) P_Z(0) \sum_t \tilde{P}_x(t) \tilde{E}_x(t) \quad (37)$$

The total number of accidents is the sum of the above functions,

$$N_a = N_{ax} + N_{ay} + N_{az} + N_{ayz} \quad (38)$$

There are a number of additional modifications which are often found in the literature and are noted below.

- (1) Occupancy, E: The occupancy represents the average number of aircraft that are proximate to one another per flight hour,

$$E_r(\text{same/opp}) = \frac{2T_r}{H}(\text{same/opp}) \quad (39)$$

The occupancy function, used in NAT SPG 4 data analysis, is a convenient function for obtaining experimental data.

- (2) Longitudinal slab dimension,  $\Lambda_x$ :  $\Lambda_x$  is often used in place of  $\lambda_x$  in order to emphasize the fact that the x dimension of the collision slab can be designed to include the effects of vortices and not just the metallic distance of the aircraft. (Note - "a vortex collision" represents one accident, not two. The equations must be so defined.)
- (3) Collision slab variable,  $\gamma$ : By multiplying the  $P_x P_y N_z$  term in the risk function by  $\gamma$  provides us with a means of altering the effective shape of the collision slab for modeling purposes.

#### IV. Parameter Evaluation

##### A. Nature of Parameter Estimates

There are a number of techniques that can be employed to obtain numerical values for the number-of-accident functions presented in Section III.

On one hand, we can select a single, "optimum" estimate for each parameter in question and then solve a deterministic equation. This "optimum" value can be defined in a number of ways. It might be the central (or average) value obtained from the observed data. Or, it could be defined in terms of confidence level statistics. (The concept of confidence levels will be briefly discussed later in this section. A more complete discussion can be found in references 2, 4, and 10.)

Alternately, we can model each parameter as a random variable by assigning to it a probability density function obtained from either empirical data or theoretical considerations. An example of this is given in Agenda Item 4, Appendix C of reference 4 where the following equation is presented:

$$\begin{aligned}
 w(N_a) = & 2k w(\text{tail area}) w(\text{tail shape}) w(\alpha) \left\{ \frac{w(T_y \text{ same})}{S_x} \left[ \frac{w(\Delta V) P_z(0)}{2} \right. \right. \\
 & \left. \left. + \frac{P_z(0) w(\Lambda_x) w(|\dot{Y}|)}{2\lambda_y} \right] + \frac{w(T_y \text{ opp})}{S_x} \left[ \overline{V} P_z(0) \right. \right. \\
 & \left. \left. + \frac{P_z(0) w(\Lambda_x) w(|\dot{Y}|)}{2\lambda_y} \right] \right\}
 \end{aligned}
 \tag{40}$$

$w(\cdot)$  indicates the fact that the parameter of interest is taken to be a random variable.  $k$  is just a scaling function and  $P_y$  is defined in terms of densities for the tail area and tail shape of the flying error distribution.  $N_a$  itself is a random variable: its density is obtained via Monte Carlo simulation. We would then calculate the probability that the number of accidents fall within specific ranges of values.

In general, the solution method used will combine both techniques. These are certain parameters we will be able to model by assigning a single estimate: the quantities  $\bar{V}$ , and  $\Delta\bar{V}$ , seem to fit into this parameter category. Other parameters, such as the overlap probabilities, will require a distributed variable approach. Therefore, the final result, is likely to be obtained via a hybrid approach using both procedures outlined above.

The remainder of Section IV is devoted to a careful tabulation of all the parameters of interest: (1) their definition (part B) and (2) their values as chosen by NAT SPG (part C).

B. Definitions

1. T<sub>y</sub> (same) [hr]: The time during which a potential hazard is assumed to exist for two aircraft flying on the same level, on adjacent tracks and in the same direction.
2. T<sub>y</sub> (opp) [hr]: The time during which a potential hazard is assumed to exist for two aircraft flying on the same level, on adjacent tracks and in opposite directions.
3. T<sub>z</sub> (same) [hr]: The time during which a potential hazard is assumed to exist for two aircraft flying on the same lateral track, on adjacent levels and in the same direction.
4. T<sub>z</sub> (opp) [hr]: The time during which a potential hazard is assumed to exist for two aircraft flying on the same lateral track, on adjacent levels and in opposite directions.
5. T<sub>yz</sub> (same) [hr]: The time during which a potential hazard is assumed to exist for two aircraft flying in the same direction on paths nominally separated by half the standard separation in both the lateral and vertical direction.
6. T<sub>yz</sub> (opp) [hr]: The time during which a potential hazard is assumed to exist for two aircraft flying

in opposite directions on paths nominally separated by half the standard separation in both the lateral and vertical direction.

7.  $\underline{H}$  [hr]: The number of flying hours over which the proximity times were calculated.
8.  $\underline{E_r}$  (same/opp): The percentage of time in which two aircraft are proximate. (r representing y or z or yz).
9.  $\underline{S_x}$  [nmi]: Dimension defining x direction proximity.
10.  $\underline{S_y}$  [nmi]: The lateral separation standard.
11.  $\underline{S_z}$  [nmi]: The vertical separation standard.
12.  $\underline{\lambda_x}$  [nmi]: The longitudinal metallic dimension of the aircraft.
13.  $\underline{\Lambda_x}$  [nmi]: The longitudinal hazard distance which includes the effect of vortices.
14.  $\underline{\lambda_y}$  [nmi]: The lateral metallic dimension of the aircraft.
15.  $\underline{\lambda_z}$  [nmi]: The vertical metallic dimension of the aircraft.
16.  $\underline{|\dot{x}|}$  [nmi/hr]: The average relative along-track speed of two aircraft during x overlap.
17.  $\underline{\bar{V}}$  [nmi/hr]: The average speed of an aircraft.
18.  $\underline{\Delta\bar{V}}$  [nmi/hr]: The average difference in along-track speed between any two aircraft.

19.  $\overline{|\dot{y}(\alpha)|}$  [nmi/hr]: The average relative lateral speed during y overlap of two aircraft, nominally separated by the lateral distance,  $\alpha$ .
20.  $\overline{|\dot{z}(\beta)|}$  [nmi/hr]: The average relative vertical speed during z overlap of two aircraft, nominally separated by the vertical distance,  $\beta$ .
21.  $\underline{P_y}(\alpha)$ : The probability that two aircraft, nominally separated by  $\alpha$  nmi in the lateral dimension, will overlap in the lateral dimension.
22.  $\underline{P_z}(\beta)$ : The probability that two aircraft, nominally separated by  $\beta$  in the vertical dimension, will overlap in the vertical dimension.
23.  $\underline{N_y}(\alpha)$  [cycles/hr]: The relative frequency with which two aircraft, nominally separated by  $\alpha$  nmi in the lateral dimension, will overlap in the lateral dimension.
24.  $\underline{N_z}(\beta)$  [cycles/hr]: The relative frequency with which two aircraft, nominally separated by  $\beta$  nmi in the vertical dimension, will overlap in the vertical dimension.
25.  $\underline{\tilde{P}_x}(t)$ : The probability of longitudinal overlap between aircraft on the same track, given on initial separation of t minutes (including Mach number correction).
26.  $\underline{\tilde{E}_x}(t)$ : The probability that two aircraft are initially separated by t minutes (including Mach number correction).

27.  $\underline{\gamma}$ : A constant parameter used to model the collision risk slab.

C. NAT SPG Parameter Values

Table I below, lists the pertinent parameter values used by NAT SPG in analyzing the results of the collision risk model. A source list is included for the reader who wishes to further investigate the rationale leading to the values chosen.

D. Overlap Probability,  $P_y(S_y)$

The overlap probability  $P_y(S_y)$  plays a central role in the analysis of the number of expected accidents,  $N_{ay}$ . It is not the purpose of this paper to provide a detailed analysis of the modeling procedures involved in ascertaining results for this parameter. More complete reviews exist elsewhere.<sup>2,4</sup> In reference 10, these relationships are applied to inertial navigation data and numerical results are presented for both the overlap probability and the expected number of accidents. For completeness, however, a cursory review of some of the more salient issues involved is deemed appropriate.

The problem of solving for  $P_y(S_y)$  can be divided into two parts. Aircraft operating on non-intersecting, adjacent tracks collide with each other as a direct result of their flying errors.



<u>Parameter</u>	<u>Units</u>	<u>Values</u>	<u>Comments</u>	<u>References</u>
$\lambda_x$	nmi	.025	Measured metallic distance of Average A/C (Vortex ignored)	Ref. 6 (p.1-23)
$\lambda_y$	nmi	.025	Measured metallic distance of Average A/C (Vortex ignored)	Ref. 7 (p.2-A-3)
$\lambda_z$	nmi	.0066	Measured metallic distance of Average A/C (Vortex ignored)	Ref. 7 (p.2-A-4)
$S_x$	nmi	120; 240	Mathematical tool only	Ref. 6 (p.1-A-19) Ref. 6 (p.1-A-20)
$S_y$	nmi	75-135	Variable for Problem	—
$S_z$	nmi	.33 (2000 ft)	Variable for Problem	—
$ \dot{z}(0) $	nmi/hr	1	Derived from FAA data (Report No. RD-64-4; 1/64)	Ref. 6 (p.4-7)
$\overline{\Delta V}$	nmi/hr	13	Average of observed data	Ref. 6 (p.1-22, p. 1-A-21)
$\overline{V}$	nmi/hr	480	Speed of average A/C considered	Ref. 4 (p.4-8)
$P_z(0)$	—	.25	Based on RAE study of IATA data (1951); cautious	Ref. 4 (p.4-10)
$N_z(0)$	cycle/hr	20 or 40	20 used for $N_{ay}$ , 40 used in $N_{ax}$ case	Ref. 6 (p.4-7)
H	hr	$1.5 \times 10^6$	Taken from 1966-1971. Used in Ref. 6 data collection scheme	Ref. 5 (p.2-A-1)
$ \dot{y}(0) $	nmi/hr	20	Correlation study of lateral speed vs. deviation from track	Ref. 6 (p.1-A-19)
$ \dot{y}(60) $	nmi/hr	47	Correlation study of lateral speed vs. deviation from track	Ref. 6 (p.1-A-19)
$ \dot{y}(90) $	nmi/hr	60	Correlation study of lateral speed vs. deviation from track	Ref. 6 (p.1-A-19)
$P_y(0)$	—	.0012	See Derivation 2 below	Ref. 7 (p.2-A-1)
$P_y(60)$	—	$11 \times 10^{-6}$	See Derivation 2 below	Ref. 6 (p.1-20)
$P_y(90)$	—	$1 \times 10^{-6}$	See Derivation 2 below	Ref. 6 (p.1-20)
$E_y(\text{same})$	—	.61	Based on data and assumption of 280 daily flights	Ref. 9 (Fig. 3)
$E_y(\text{opp})$	—	.01	Based on data and assumption of 280 daily flights	Ref. 9 (Fig. 4)
$E_z(\text{same})$	—	.73	Based on data and assumption of 280 daily flights	Ref. 9 (Fig. 5)
$E_z(\text{opp})$	—	.02	Based on data and assumption of 280 daily flights	Ref. 9 (Fig. 6)
$E_{yz}(\text{same})$	—	1.46	Assumed to be twice $E_z(\text{same})$ ; cautious	Ref. 7 (p.3-A-4)
$E_{yz}(\text{opp})$	—	.04	Assumed to be twice $E_z(\text{same})$ ; cautious	—
$E_x(t)$	—	.014 for all $t > t_{\min}$	Very rough estimate	Ref. 7 (p.4-A-6)

TABLE I.- NAT SPG Parameter Values

The first step, then, is to model the flying-error density. The second step is to relate this error density to the overlap probability itself.

Bypassing the first step for a moment, the relationship between position errors and the overlap probability is treated in derivation 2 below.

#### DERIVATION 2

We consider two aircraft on adjacent tracks of a parallel track system. Each aircraft has associated with it a probability density describing its position error. (For the moment, these densities are considered known.) This situation is depicted in Figure 7 (where  $r$  may be considered the lateral dimension.)

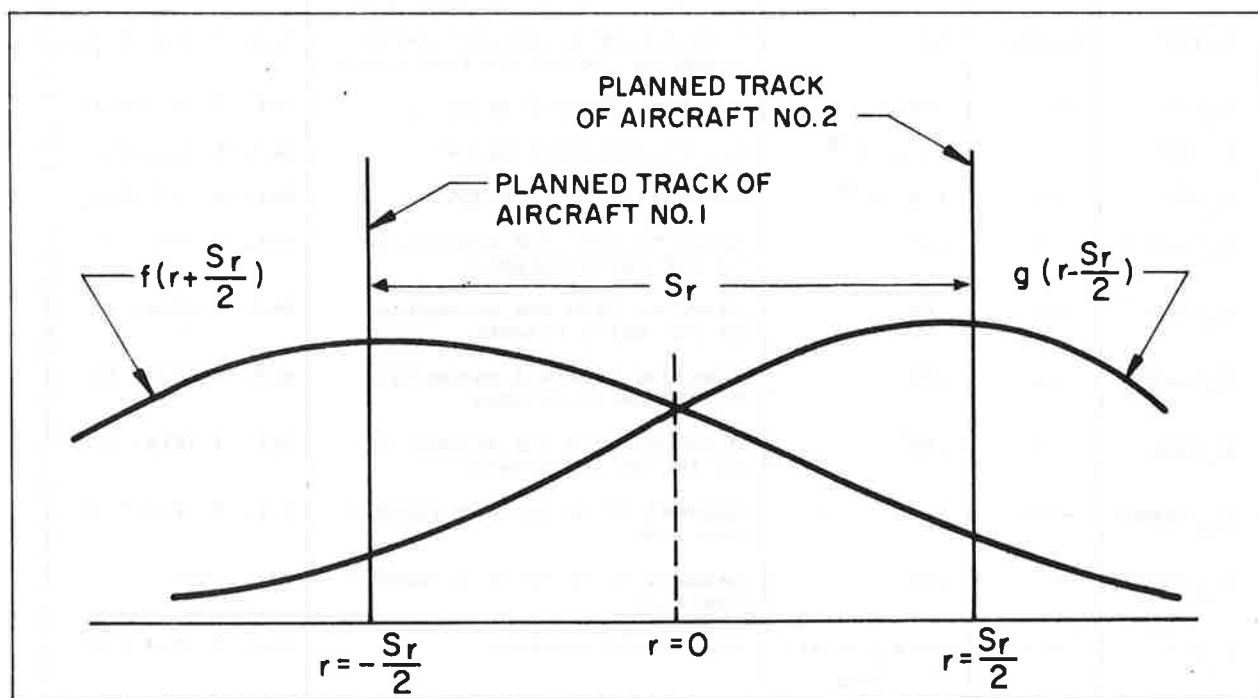


Figure 7.- Probability Density of Aircraft Position Errors

The probability that the center of aircraft No. 1 lies between  $r$  and  $dr$  is:

$$f(r + S_r/2) dr.$$

Each aircraft is assumed to span a distance  $\lambda_r$  in the  $r^{\text{th}}$  dimension. The probability of overlap, given that the aircraft No. 1 is centered at  $r$ , is simply the probability that aircraft No. 2 is centered somewhere between  $r - \lambda_r$  and  $r + \lambda_r$ . The probability of this occurrence is:

$$\int_{r - \lambda_r}^{r + \lambda_r} g(\mu - \frac{S_r}{2}) d\mu$$

The probability that the two aircraft overlap at  $r$  is simply the product of these two functions.

$$\left\{ \begin{array}{l} \text{Probability of overlap} \\ \text{at } r \end{array} \right\} = f(r + \frac{S_r}{2}) dr \int_{r - \lambda_r}^{r + \lambda_r} g(\mu - \frac{S_r}{2}) d\mu \quad (41)$$

The total probability of overlap is obtained by integrating equation (41) over the whole space.

$$P_r(S_r) = \int_{-\infty}^{\infty} f(r + S_r/2) \int_{r - \lambda_r}^{r + \lambda_r} g(\mu - \frac{S_r}{2}) d\mu dr \quad (42)$$

Assuming that (1)  $g(r)$  is essentially constant over distance  $2\lambda_r$  and (2) that both aircraft have identical densities (i.e.,  $f(r) = g(r)$ ), we obtain:

$$P_r(S_r) = 2\lambda_r \int_{-\infty}^{\infty} f\left(r + \frac{S_r}{2}\right) f\left(r - \frac{S_r}{2}\right) dr \quad (43)$$

Therefore, the overlap probability is the self convolution of the assumed position error density.

This leaves one remaining question, namely the one posed in step one. How do we model the position error density from observed data? In order for a collision to occur between two aircraft operating on parallel, adjacent tracks, at least one aircraft must deviate from track center by a distance in excess of  $\frac{S_r}{2}$ . It is this large, relatively infrequent error that plays the dominant role in equation (43). The density function is divided into two parts: (1) the body defined between  $-\frac{S_r}{2}$  and  $\frac{S_r}{2}$  and (2) the tail defined from  $\frac{S_r}{2}$  to  $\infty$  and from  $-\infty$  to  $-\frac{S_r}{2}$ .

Modeling the body poses no problem, in general. Since most of the observed data lies in the body, fitting a curve to the data in this region is straightforward. Furthermore, the final result can be shown to be relatively insensitive to body shape.

Based on the data collected for its fourth meeting (reference 6), NAT SPG has chosen a First-Laplacian (or double-sided exponential) density to model the body.

$$f(r) = \frac{1}{\sqrt{2}\sigma_r} e^{-\sqrt{2}|r|/\sigma_r}, \quad |r| \leq \frac{s_r}{2} \quad (44)$$

A preliminary study of INS data indicates a Gaussian density might provide an optimum body shape.

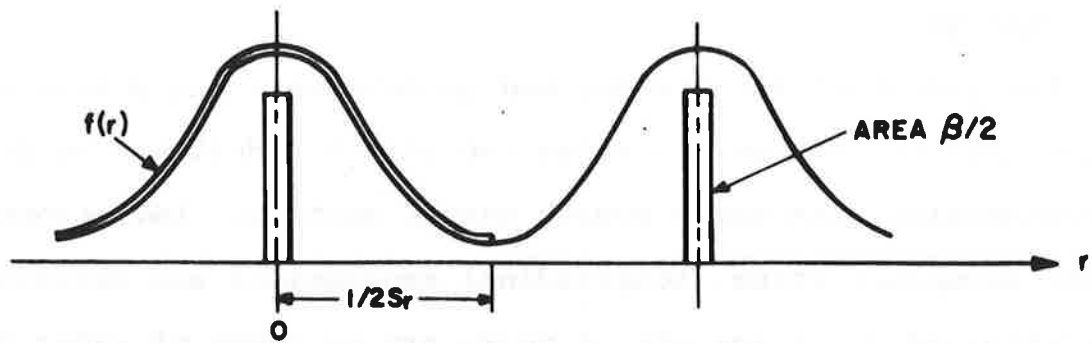
The real problem lies in modeling the sparsely populated tail area. According to P.G. Reich, "The incidence of large, rare flying errors cannot safely be deduced by simple theories which extrapolate from small samples ... special statistical techniques have to be used to estimate ... " the tail, both in area and in shape. In essence, the question involved in estimating the tail area reduces to: what "confidence" can one place on estimating the occurrence of a rare event from a limited sample of data? This difficulty is dealt with by means of confidence level statistics. One attempts to choose assumptions in order to insure that, where there is reason to be in doubt, a high estimate is obtained. We, therefore, overestimate the tail area and, in doing so, obtain "confidence" that should we err, we will err on the safe side. In other words, we try to be conservative.

Once we have chosen a tail area, we must model the tail shape. Reich<sup>2</sup> considers three possible assumptions: (1) the "pessimistic spike", which places the entire tail area at the

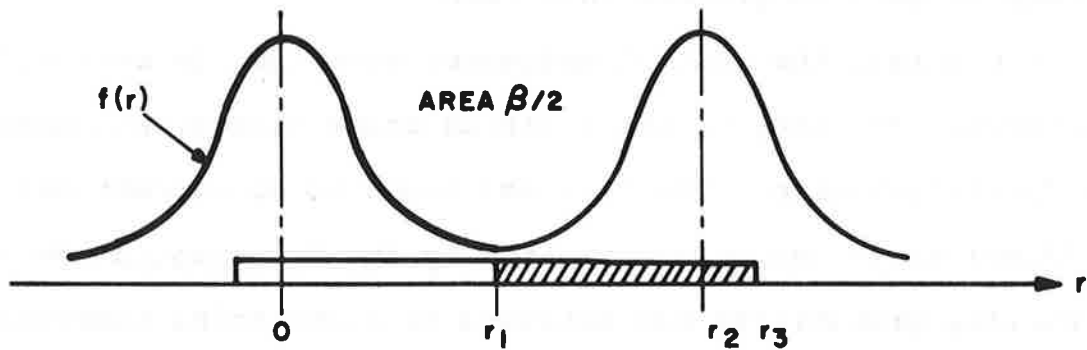
center of the adjacent track, (2) the "level tail", and, (3) the "exponential decay". These three cases are depicted in Figures 8(a-c).

The assumption chosen is a critical one. We wish to be conservative. At the same time, there is a danger in being so conservative as to derive unreasonable and unrealistic requirements. For the same tail area,  $\beta$ , it can be shown that the collision risks derived from these three assumptions can vary by a ratio of 100: 20: 1 ! (This result is even more incredible when one realizes that the overlap probability is only one of many parameters to be estimated. As much as a 6000: 1 ratio in the collision risk can result between pessimistic and optimistic assumptions for each parameter<sup>4</sup>.)

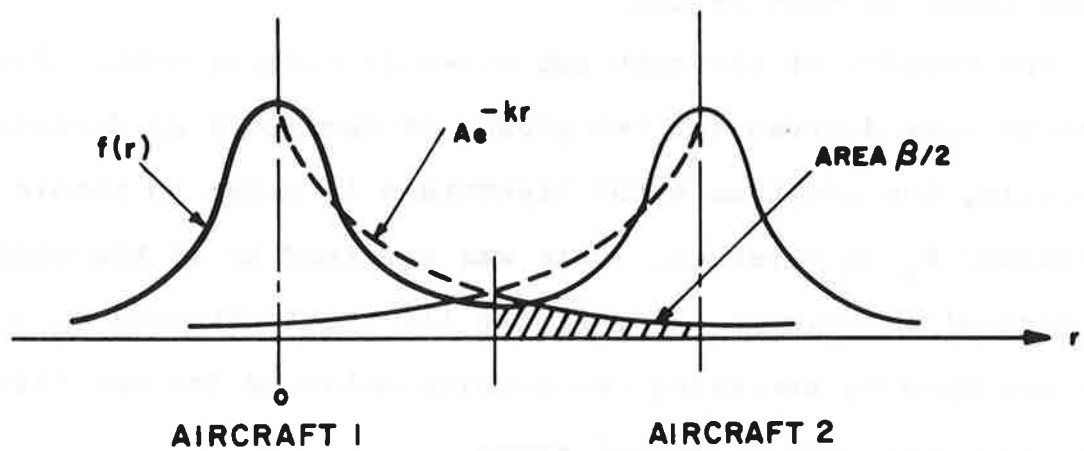
The NAT SPG data<sup>6</sup> was best modeled by a compromise between a level and an exponential tail. The INS data, currently being analyzed, appears to be at least as good as an exponential tail. There is reason to believe that even a Gaussian density (body and tail) may be appropriate.



(a) "PESSIMISTIC SPIKE" ASSUMPTION



(b) "LEVEL TAILS" ASSUMPTION



(c) "EXPONENTIAL DECAY" ASSUMPTION

Figure 8.- Alternative Assumptions of Tail Shape

## V. Results

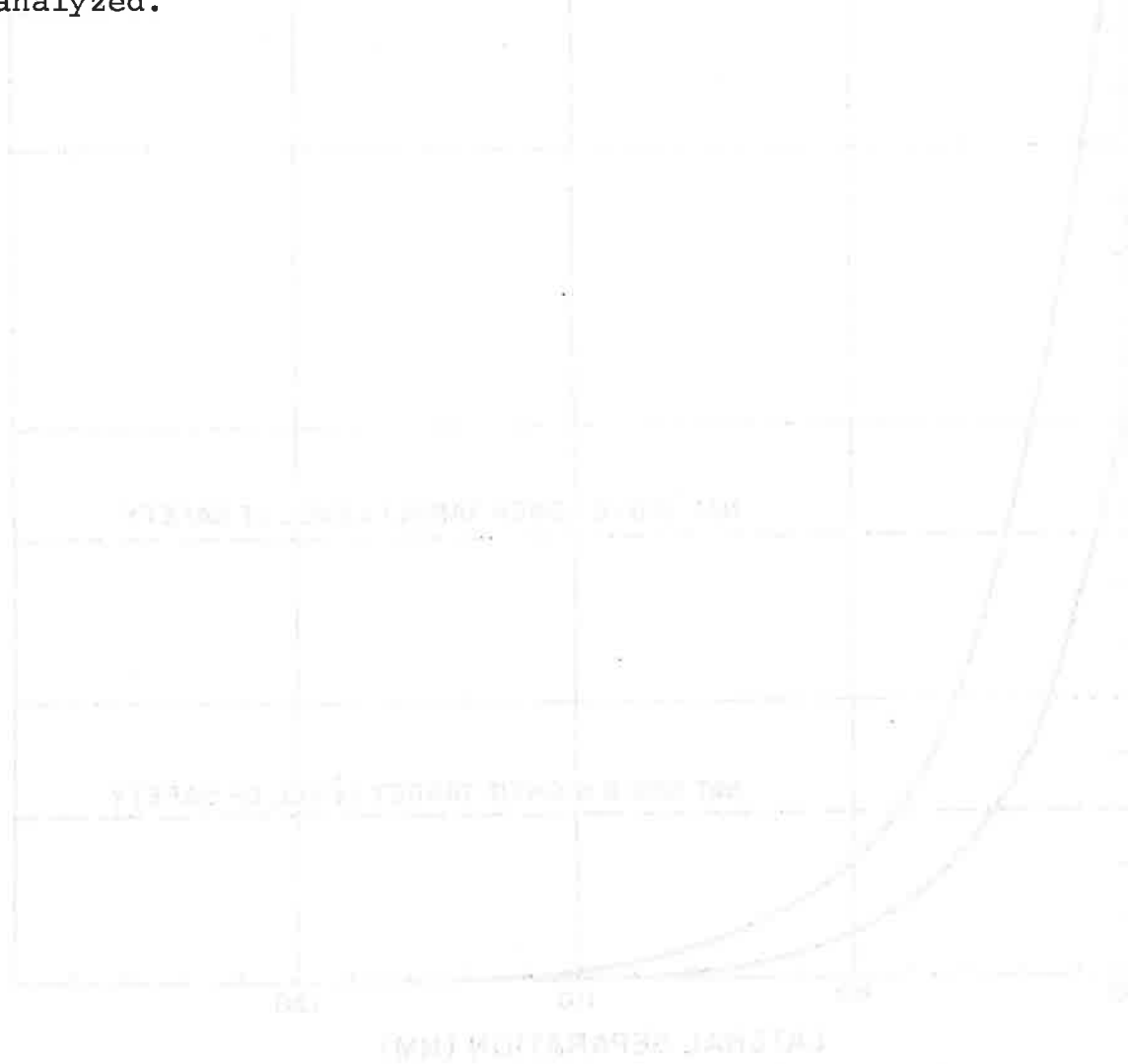
The principal results derived to date were the direct result of the data collection and reduction effort undertaken by NAT SPG in conjunction with their fourth annual meeting. Deviations from track, occupancy rates, longitudinal separations and velocities were obtained for a variety of operators by means of radar fixes from six key locations. Appendix A of the NAT SPG 4 proceedings<sup>6</sup> presents the data obtained. Item 1 of the same report details the methods used to process this data.

In general, the central estimates were used in estimating parameters. The body of the position error density was modeled by a first-Laplacian. The tail was shown to be overestimated by the "level tail" and underestimated by the "exponential decay". The overlap probability was obtained by calculating individual overlap probabilities for various regions of the ocean and taking a weighted sum of the results in accordance with the relative flying times in each region.

The results of interest are shown in Figures 9-11. Figures 9 and 10 were derived for two groups of operators by directly convolving the position error histograms in order to obtain the individual  $P_y(S_y)$  values. This was referred to as the central (or "actual") estimate. For Figure 11, the individual  $P_y(S_y)$ 's were obtained by averaging the results obtained for the "level tail" and "exponential decay" cases.



Additional results, based on the NAT SPG 4<sup>6</sup> data collection effort, were tabulated in NAT SPG 6,<sup>8</sup> Agenda Item 3 for a composite system. Here, values were presented for the "optimistic" and "pessimistic" assumptions concerning  $N_{ay}$ ,  $N_{az}$ ,  $N_{ayz}$  and  $N_{ax}$ . The results are indicated in Table II. In addition, the effect of flight level changes on the number of expected accidents was analyzed.



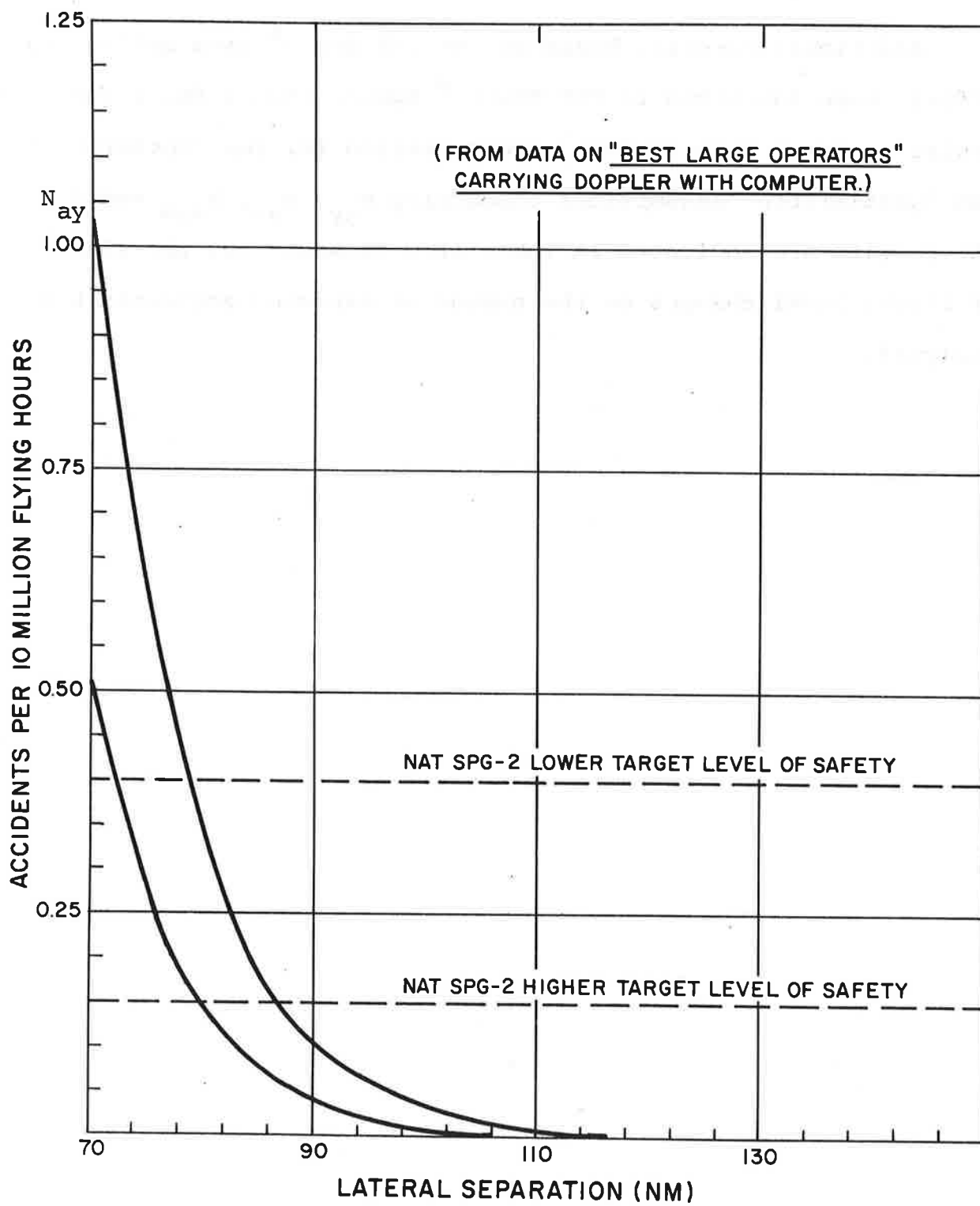


Figure 9.-  $N_{ay}$  vs  $S_y$  [NAT "Central" Estimates]

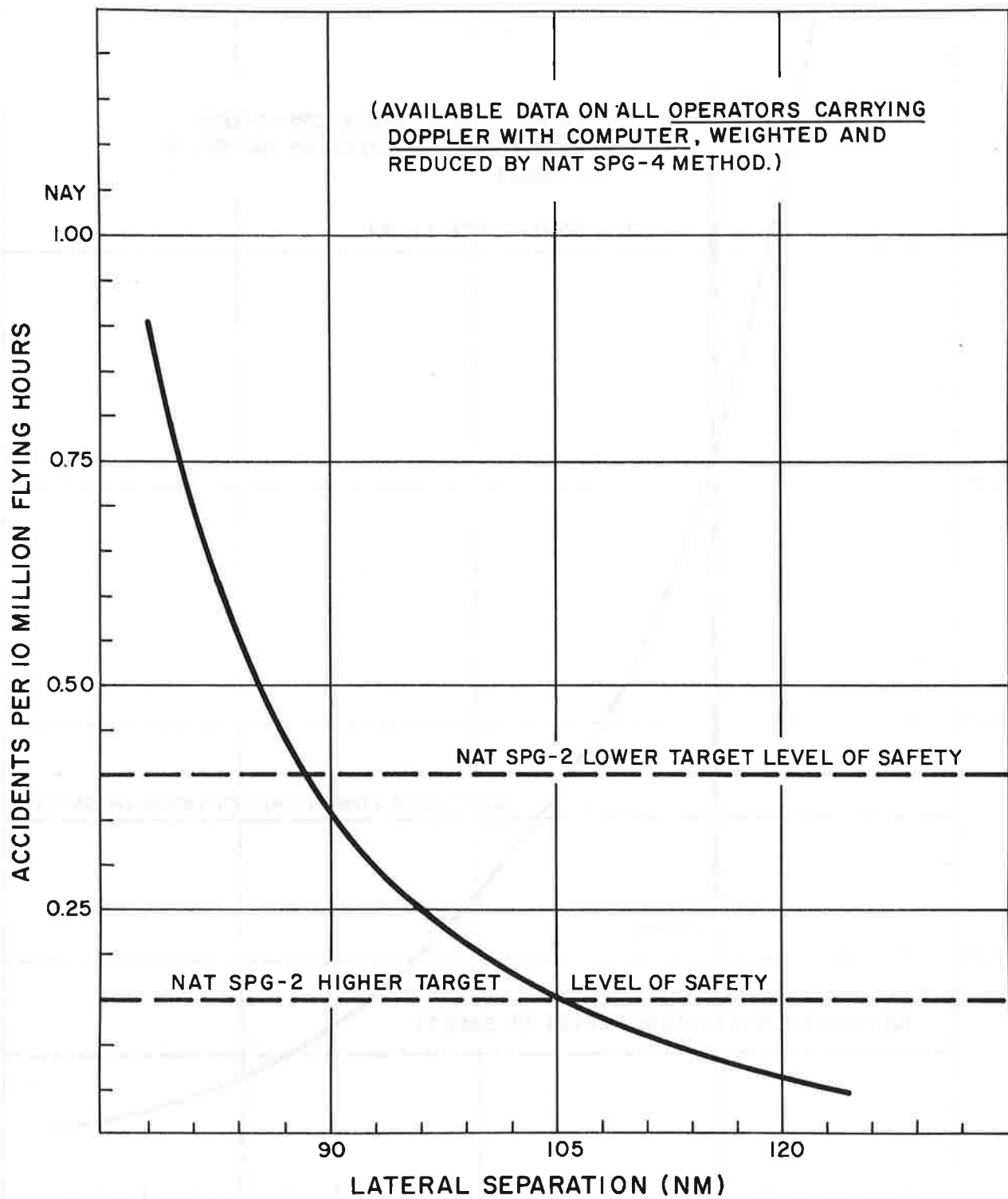


Figure 10.-  $N_{ay}$  vs  $S_y$  [NAT "Central" Estimates]

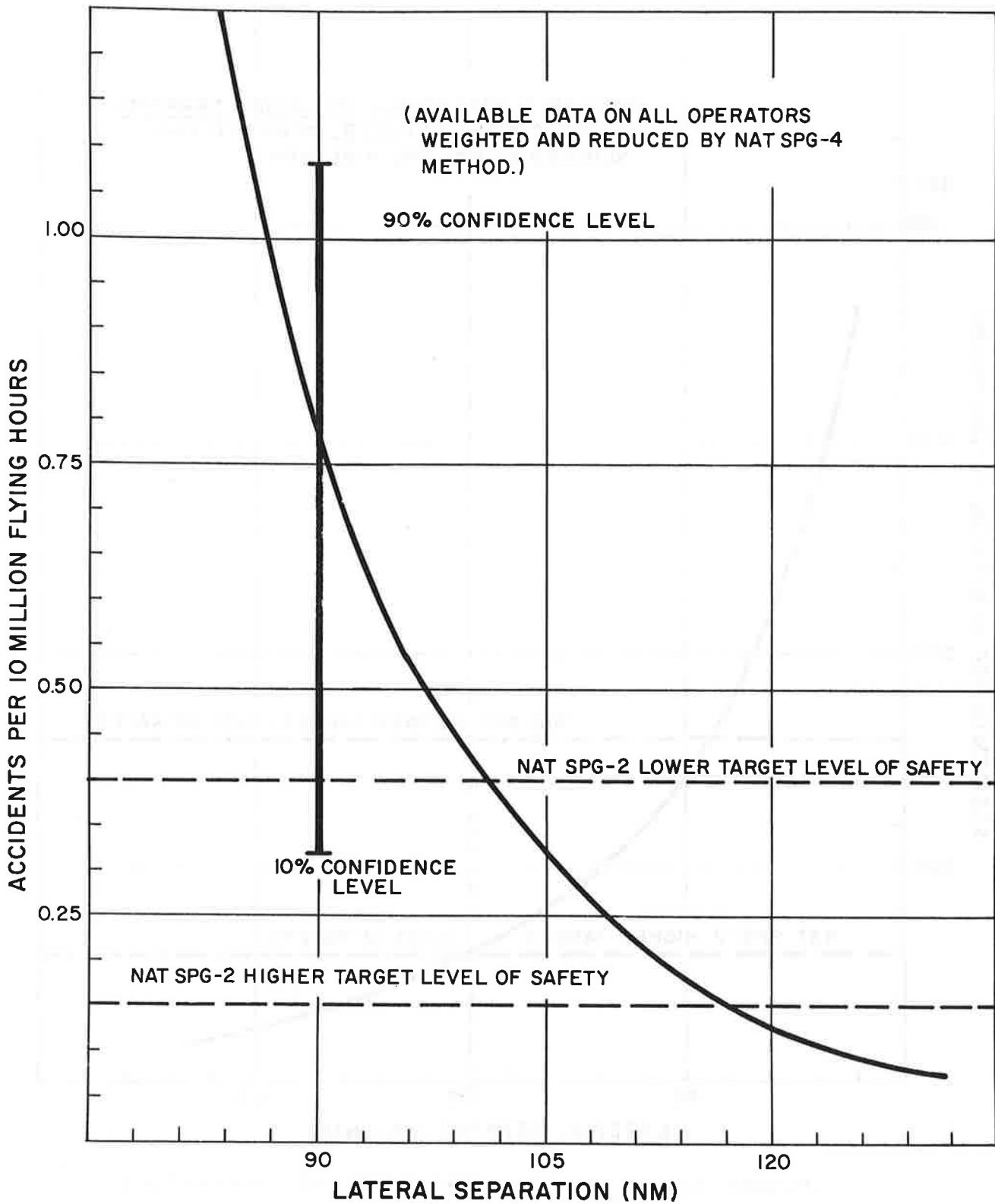


Figure 11.-  $N_{ay}$  vs.  $S_y$  [NAT SPG 4 Method]

Accident Functions ( $10^7$ Hour Flying)	"Best Estimate"	"Cautious Estimate"
$N_{ay}$ (120 nm)	0.11	0.18
$N_{az}$ (2000 ft)	0.02	0.05
$N_{ayz}$ (60 nm + 1000 ft)	0.03	0.04
$N_{ax}$ ( $t_{min} = 15$ min)	0.05	0.15
FLIGHT LEVEL CHANGES	0.01	0.02
TOTAL, $N_a$	0.22	0.44

TABLE II.- NAT SPG Results

Finally, the reader is directed to reference 12 for a review of a preliminary set of results based on an inertial navigation system data base.

## VI. Conclusions & Recommendations

1. The collision risk calculation should be extended to consider navigation systems that are time and location dependent. This is particularly true in the case of aircraft carrying INS or Doppler navigation systems. A first-cut effort in this direction has been made and is reviewed in reference 10. More work in this area is expected in FY72.

2. A full study of the collision risk associated with a satellite Air Traffic Control Surveillance System is called for. Both in-house and out-of-house work is planned in this area.

3. A great deal of work is still required in the area of parameter estimation. This effort should concern itself with a number of issues including (1) updating those parameters associated with new systems, (2) testing the sensitivity of the risk function to a variety of individual parameters, and (3) calculating the output confidence level as a function of the confidence levels of the input parameters.

4. The solution methods should be refined in order to facilitate risk calculations in a mixed air space. The procedure used to date has been to model each parameter once (either as some central estimate or distributed variable by using an averaging technique. A study should be made of multiple estimate techniques. For example, consider an airspace consisting of 60% Boeing 707's with Doppler Navigation and 40% Boeing 747's with redundant INS systems. Two sets of parameters should be specified and the

expected number of accidents should be calculated on the basis of a probabilistically weighted average of the risks resulting from 707-707, 707 747 and 747-747 proximities.

5. Even though many modeling issues remain to be resolved, the results given in Table II (page 47) are quite significant, particularly in regard to the relative values between the composite risk and the lateral risk. The addition of diagonal paths, while nearly doubling system capacity, has a minimal effect on system safety. Even the "cautious" estimate of the sum falls within the lower target level of safety ( $N_a = .45$ ) as agreed upon in NAT SPG 2<sup>4</sup>. Hence, the composite system is proven to be a viable concept.

6. Even though the opposite-directed traffic accounts for 3% of the proximity time encountered in trials, it results in 42% of the expected accidents<sup>9</sup>. Attention should be centered on possible segregation schemes for opposite directed flow.

7. The size of the available sample data is insufficient for assessing, with any confidence, the present risk levels in the longitudinal case. Investigation should be made into the use of DME to shorten the across track spacing (possibly to 9 minutes).<sup>6</sup>

8. Based on NAT SPG 4<sup>6</sup> (non-INS) data, a lateral standard of 90 nmi will not be uniformly safe. The "best" (Doppler) users can safely use 90 nmi, but other carriers, with less accurate NAV systems, will be unable to do so with sufficient

safety.<sup>6</sup> This problem of widely varying requirements will become amplified as INS carriers enter the system. Perhaps a penalty assessment scheme can be applied to "weak links" in terms of suboptimal routes. This would be a viable concept only if the operational problems of such control were held to a minimum.

9. There is insufficient evidence now to justify 1000 ft vertical separations on identical tracks.<sup>8</sup>

10. More work is required in the area of assessing the effects of enroute level and track changes.

11. The confidence level technique for estimating the tail areas of the position error density may give unduly pessimistic results when there are a very small number of observations in the tail. These cases require further investigation.



## VII. References

1. "Analysis of Long-Range Air Traffic Systems: Separation Standards - I", P. G. Reich, Journal of the Institute of Navigation, Volume 19, No. 1, January 1966.
2. "Analysis of Long-Range Air Traffic Systems: Separation Standards - II", P. G. Reich, Journal of the Institute of Navigation, Volume 19, No. 2, April 1966.
3. "Analysis of Long-Range Air Traffic Systems: Separation Standards - III", P. G. Reich, Journal of the Institute of Navigation, Volume 19, No. 3, July 1966.
4. "Summary of Discussions of the Second meeting of the NAT Systems Planning Group", December 1966.
5. "Summary of Discussions of the Third Meeting of the NAT Systems Planning Group", April 1967.
6. "Summary of Discussions of the Fourth Meeting of the NAT Systems Planning Group", June 1968.
7. "Summary of Discussions of the Fifth Meeting of the NAT Systems Planning Group", December 1968.
8. "Summary of Discussions of the Sixth meeting of the NAT Systems Planning Group", September 1969.
9. "Studies of Traffic Packing for Estimating Mid-Air Collision Risk over the North Atlantic", P. P. Scott, Royal Aircraft Establishment Technical Report 68097, April 1968.

10. "The Impact of Inertial Navigation on Air Safety", R. M. Hershkowitz, D. O'Mathuna, K. R. Britting, presented to Institute of Navigation, April 14, 1971 (also issued as a TSC Technical Report).